

Engineering investigation of the Kensey dynamic angioplasty catheter

P. Godlewski, M. Nagurka and M. Wholey*

Department of Mechanical Engineering, Carnegie Mellon University, Pittsburgh, PA 15213, USA; *Department of Radiology, Shadyside Hospital, Pittsburgh, PA 15232, USA

Received July 1990, accepted March 1991

ABSTRACT

This article describes an in vitro experimental study which was designed to gain a better understanding of the mechanism by which the Kensey catheter mediates atherosclerotic tissue. The major goals of the study were to observe the generation of debris particles during revascularization and to elucidate the fluid dynamic effects associated with particle motions at and around the tip of the catheter. To investigate these phenomena, in vitro actual size and large scale model experiments were conducted. The results of these experiments provide a reference for the significance of the clinical performance of the Kensey catheter.

Keywords: Kensey catheter, atherosclerotic tissue, distal embolization, revascularization

INTRODUCTION

Angioplasty – the dilation of a partially occluded artery by the inflation of a balloon catheter – serves as an effective method for restoring blood flow through arteries of the heart and peripheral vascular systems that are narrowed as a result of atherosclerosis. Traditionally, revascularization of such arteries has depended on vascular surgery. Angioplasty has significant advantages relative to surgery since it is less invasive and less costly. Limitations exist with the procedure since the balloon catheter must be introduced through existing passageways leading through the constricted area and the length of the constriction may greatly exceed the length of the balloon.

In recent years, new catheters have been introduced to mediate total occlusions and long stenotic lesions. Some of these catheters employ lasers that burn away atherosclerotic tissue by direct contact with a heated distal tip or by direct illumination. Other catheters mechanically mediate the diseased tissue. For example, some catheters shave away diseased tissue; others rotate at high speeds grinding plaque away from the artery wall. The Kensey dynamic angioplasty catheter (manufactured by Theratek International, Inc. and distributed by Cordis Corporation, Miami Lakes, Florida) belongs to the latter category of revascularization devices.

The Kensey catheter is a device designed to revascularize percutaneously, partially and fully occluded atherosclerotic arteries by direct mechanical intervention. It consists of a bladed tip exposed at the distal end of a flexible cable inside a catheter. Driven by a DC servo motor, the tip rotates at speeds

close to 100 000 rpm. (Figure 1 shows a photograph of the Kensey catheter tip.) A fluid injector system provides the catheter with perfusate which exits behind the rotating tip acting as a source of lubrication for the drive cable as well as a means of heat dissipation. In order to ensure clear downstream passage, plaque must be mechanically reduced into particles of the order of $7\ \mu\text{m}$ in diameter¹. These particles can then pass without effect through the microvasculature to be filtered out from the blood supply. This requires that the Kensey catheter micropulverizes plaque to avoid blockages further along the bloodstream.

Studies in Europe of the Kensey catheter, used on 111 patients, report a clinical success rate of 80%²; other studies report a 0.7% incidence of clinically significant distal embolization, i.e., downstream occlusion resulting from particulate debris³. Minimal micropulverization was observed in investigations⁴ of the Kensey catheter in fresh, above knee amputated legs. These studies demonstrated that the 'majority of particles were much larger than the size of red blood cells ($7\ \mu\text{m}$), ranging from a few micrometres up to 2 cm in length'. Dr Kensey also reported *in vivo* evidence of embolization⁵.

This report describes *in vitro* experiments conducted to investigate Kensey catheter performance in the mediation of atheroma. The study has been designed to observe and analyse the generation of debris particles and follow their subsequent trajectories to elucidate the fluid dynamic effects associated with particle motions that are necessary for pulverization. Actual size and large scale ($10\times$) model experiments were conducted *in vitro* and performance data, including photographic evidence of particle motions and fluid flow, were recorded. The results of these

Correspondence and reprint requests to: Professor M. Nagurka

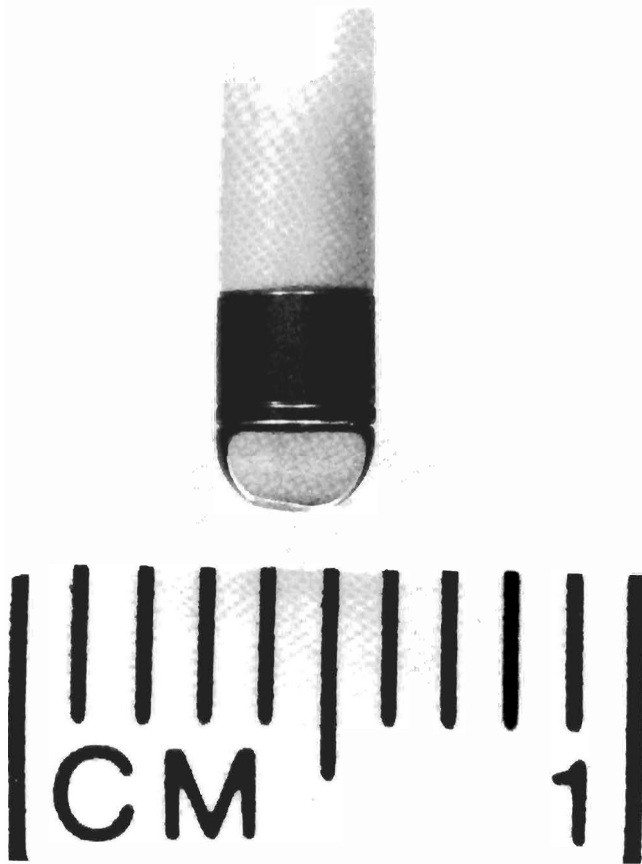


Figure 1 Photograph of 8 French Kensey catheter tip (side view)

experiments provide a reference for the assessment of the actual performance of the Kensey catheter.

DESCRIPTION OF THE KENSEY CATHETER

The Kensey catheter consists of an approximately hemispherical tip connected inside a thrust/journal bearing assembly to a stainless steel cable, 1.2 m in length. The cable acts as a torsional spring between the drive system and the tip. If the tip rotation is arrested, the drive system can continue to rotate until torsional failure of the cable. A DC motor rotates the cable inside a flexible polyurethane sleeve with a 2.67 mm outer diameter. Exposed at the tip is a forward cutting edge with a variable, negative rake angle. The catheter is guided without the aid of supplementary guidewires which are necessary in balloon angioplasty to track balloons across the diseased area. This enables the use of the Kensey catheter in totally occluded arteries where it might not be possible to introduce a guidewire.

Perfusate flow is injected at the proximal end of the catheter and exits through channels engraved in the thrust bearing at the catheter tip. If the perfusate pressure becomes too large, the drive control system automatically stops the catheter from rotating. When the catheter tip rotates the perfusate sprays radially from behind the catheter tip.

Methodology

In vitro experiments were conducted to permit observation of the actual catheter's performance in different materials representative of atheromatous plaque. These experiments were designed to visualize the generation of model particulate debris and follow its motion about the tip. Operational variables such as tip speed, perfusate injection rate, and tip advance speed were varied. Videotape recordings were made to acquire evidence of particle generation and to monitor flow and recirculation of particles at and around the catheter tip. Although these experiments helped to elucidate the complex fluid dynamic behaviour of model particulate material, the small size of the catheter tip and its high speed complicated visualization. To provide a more complete visualization of the flow surrounding the tip, a 10× scale, dynamically representative model of the catheter was constructed. The 10× scale model was an effective tool in clarifying fluid dynamic behaviour. The following are results of both the actual size and 10× scale catheter experiments.

EXPERIMENTAL PROCEDURES

Actual catheter experiments

In tests using the actual catheter, arteries were simulated using tygon tubing or glass tubing with an 8 mm inner diameter, similar in size to the inner diameter of the femoral artery. Water, a Newtonian fluid, at room temperature (20°C) was used to simulate blood. Although blood is a non-Newtonian fluid for shear rates less than 10 s⁻¹, it acts as a Newtonian fluid at rates corresponding to *in vivo* conditions⁶. Two remotely controlled DC pumps, connected to either end of the tubing, were used to

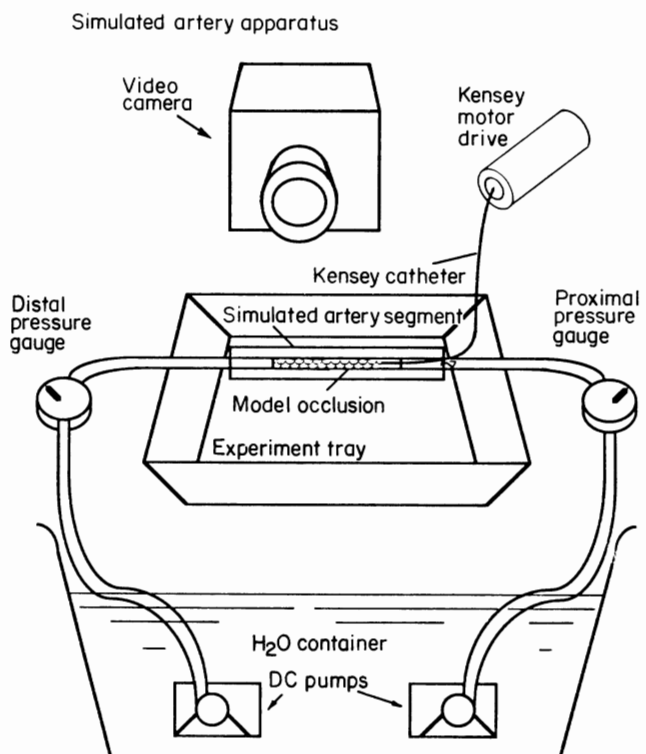


Figure 2 Schematic of actual size experimental set-up

establish a pressure gradient across model occlusions. Pressure differences of the order of 0.014 N mm^{-2} (2 psi) were employed, since such drops occur across occlusions in peripheral arteries⁷. Figure 2 shows a schematic of the experimental set-up.

Different materials (different density gelatin, cheeses, animal fats) were used to permit an evaluation of catheter performance in fibrous, binding materials as well as soft, elastic materials as those represented by Dr Kensey's study⁸. A standard, surrogate material for *in vitro* models of atheromatous material has little reference, so materials were evaluated for their consistency and compared to atherosclerotic plaques found in freshly excised, cadaveric arteries. Of all the materials considered, gelatin was chosen for studies visualizing particulate generation because of its transparency and facile preparation. Gelatin was prepared within a narrow range of densities (0.00101 to 0.0011 g mm^{-3}), close to water, and was coloured to aid in discerning particulate formation. Silicon sealant and paraffin wax were also considered as potential clot materials. Silicon sealant was tested because it has viscoelastic properties and is transparent. However, it was not used for visualization studies because a tough skin formed on the ends of the model clot which was difficult to penetrate with the catheter tip. Paraffin is hard and dense, and proved to be too opaque for any recordable visualization. In summary, although major limitations exist in constructing an atheroma model, gelatin was selected since it is soft enough for the catheter to penetrate and is transparent, enabling direct visualization.

The gelatin model occlusions were 25 to 50 mm in length and were held in place primarily by adhesion of the gelatin to the inner surface of the tubing. In addition, they were mechanically locked in place between tubing sizes. Figure 3 shows a model occlusion locked in place by concentric tubing. The catheter was introduced into the tubing 50 to 130 mm proximal to the occlusion. Shorter distances were not representative of *in vivo* situations. For distances larger than 130 mm, frictional resistance of the catheter sleeve contacting the tygon tubing wall impeded the advance of the catheter.

In these visualization studies, feed rates, tip speeds, and gelatin occlusion densities were systematically varied. The catheter was operated at various tip speeds ranging from 20 000 to 90 000 rpm, the lower and upper limits of the catheter's operating speed, respectively. A maximum free speed of the catheter tip was found to be 93 000 rpm ($\pm 3\%$). The tip speed was monitored via a stroboscope to ascertain consistency with the metered reading of the drive unit

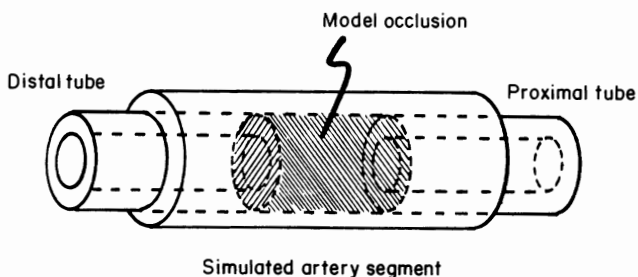


Figure 3 Schematic of model occlusion locked in place by concentric tubing

(model KC0). One side of the catheter tip was striped to enable visualization when the tip speed was synchronized with the stroboscope. The perfusate flow rate was 20 ml min^{-1} throughout the visualization experiments. The catheter passed through the model occlusions using different methods of advance. The manufacturer recommends that the operator advance the tip through a lesion by alternately pushing the catheter forward and retracting it slightly⁹. When the tip was pushed through the lesion in one continuous motion, average feed rates in gelatin occlusions were 2.4 mm s^{-1} . In other tests with occlusions made from cheeses, feed rates were varied from 5 to 10 mm s^{-1} . The catheter sleeve adhered to gelatin more effectively than to cheese which impeded its advance.

The fluid dynamic behaviour at the tip was documented using various CCD video cameras with 13 mm ($1/2$ inch) and 19 mm ($3/4$ inch) recording equipment. Because of the high speeds of the catheter, it was difficult to follow the precise movements of particles. Individual images of moving particles were often blurred. This problem was overcome by implementing a form of continuous stop action photography in which a stroboscope was synchronized with the equivalent shutter speed of a high resolution black and white CCD video camera. The flash durations of the stroboscope, of the order of 0.1 ms, enabled stop action photography with every frame of the video recording. For experiments with the actual catheter, the time between each frame accounted for three to four revolutions of the catheter tip at high speeds. Slow motion replay of individual frames enabled observation of actual particulate recirculation, which was monitored by tracking the movement of discrete particles from model occlusions during recanalization. Figures 4 and 5 show photographs of the catheter tip in model occlusions taken as individual frames of the video recording.

A total of 30 experimental tests were conducted in gelatin occlusions using the actual catheter. An additional ten tests were conducted in cheeses and animal fats.

10 × Scale catheter experiments

Visualization and analysis of fluid flow pertaining to particulate recirculation in an existing lumen was

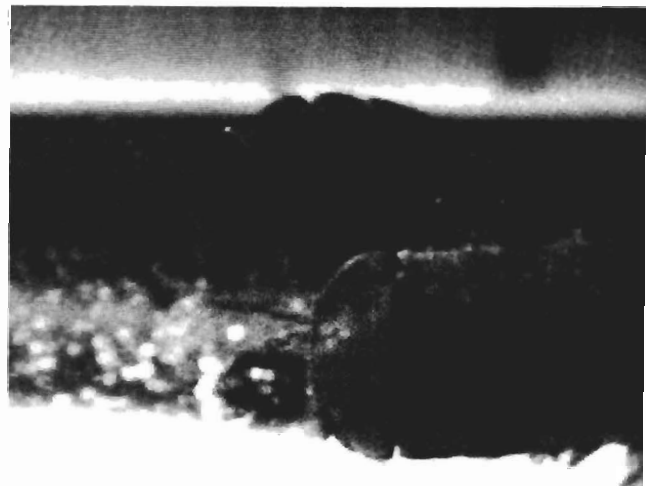


Figure 4 Stop action photograph of Kensey catheter operating in model occlusion (evidence of particle generation)

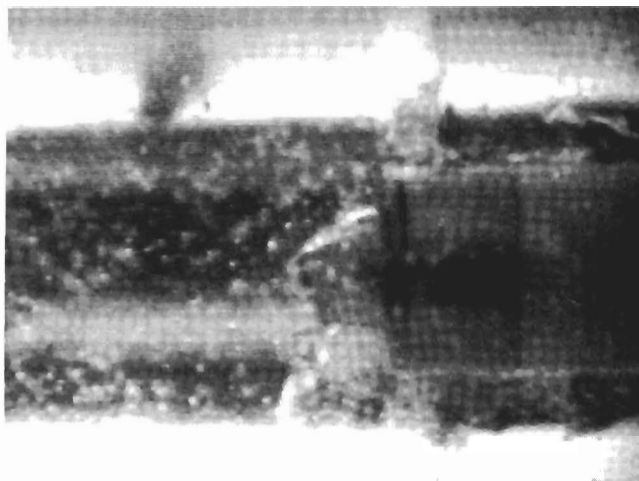


Figure 5 Stop action photograph of Kensey catheter operating in model occlusion (evidence of bubble formation due to perfusate and dynamic effects)

approached using a dynamically similar but enlarged model of the catheter. Theratek International, Inc. supplied a 10× geometrically scaled model of the catheter tip. It was rotated at the end of a 305 mm length of aluminum pip by an AC asynchronous motor via a steel shaft and flexible coupling. This catheter assembly was designed to operate vertically inside a water-filled visualization chamber, a transparent cylindrical tube with a 100 mm inner diameter, which was suspended from a reservoir tank.

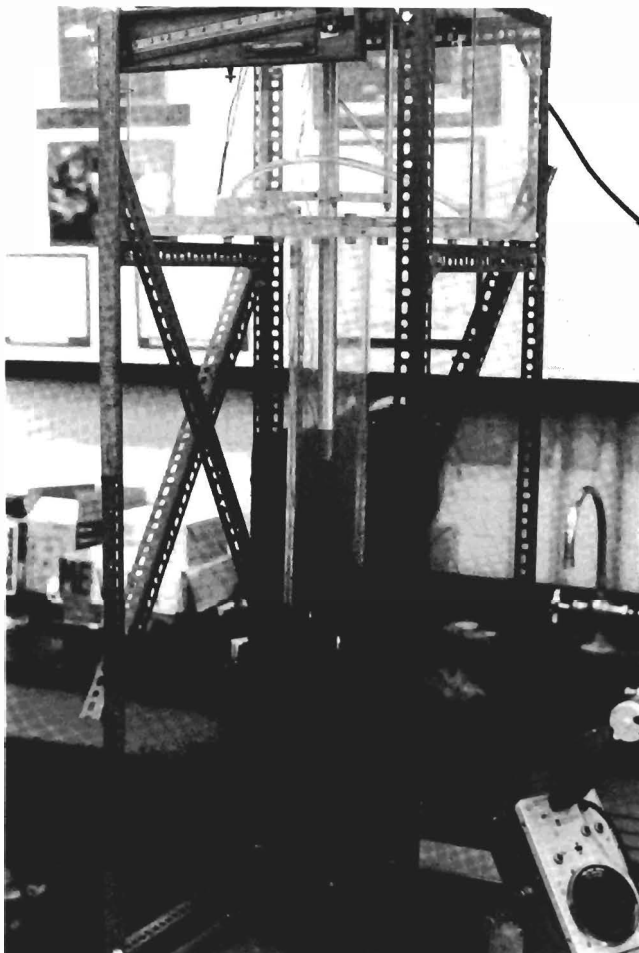


Figure 6 Photograph of 10× geometrically scaled catheter apparatus used in visualization experiments

Figure 6 shows a photograph of the 10× scale apparatus. The catheter model was designed to be displaced radially, thus simulating the centred as well as off-centred positions of an actual catheter tip in an artery. Two pumping systems were installed. One DC pump was used to fill the visualization tube and tank as well as to superimpose a net flow through the cylinder in order to simulate blood flow in an artery. Another DC pump was used to inject the catheter with water to model the perfusate flow. The tip speed of the 10× scale catheter was 900 to 1000 rpm, which was dynamically representative of an actual tip speed of 90 000 to 100 000 rpm. Gelatin particles which were close to neutrally buoyant were introduced proximally in the reservoir tank. As they drifted down near the tip, these particles were photographed and videotaped to monitor fluid flow patterns. Using the 10× scale apparatus, over 40 experimental tests were conducted.

DISCUSSION

Fluid dynamic effects

When the catheter is introduced into an actual occlusion, fluid (blood and injectate) is trapped in a small volume around the catheter tip. Since injectate is continuously pumped in, it will expand the cavity and/or it will disperse proximally through the section of lesion already opened. Figure 5 shows an example of perfusate bubble formation. *A priori*, it is unknown which of these events will occur. Typically, when the catheter operates in an occlusion, fluid shear rates become large because the tip is close to boundaries, i.e., to occlusion material in front of the tip. Large shear rates may induce turbulence in the surrounding fluid, complicating analysis of fluid movement in this region. Since particles are in the proximity of these boundaries, it is also difficult to predict their movement.

When the catheter is outside an occlusion, the geometry surrounding the tip is relatively stable, and it is possible to model the flow. When spinning in a cylinder (an approximation of the interior of an artery) the tip of the catheter generates two superimposing fluid dynamic effects. The primary flow is a vortex spinning around the longitudinal axis of the cylinder. Figure 7 shows a schematic view of the primary flow vortex. The secondary flow is an annulus of vortices along the longitudinal axis that

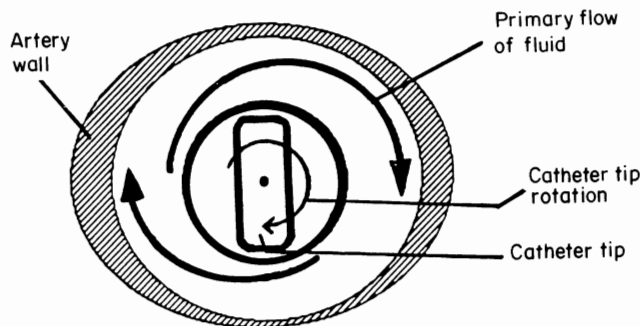


Figure 7 Head-on schematic view of Kensey catheter tip showing primary fluid vortex

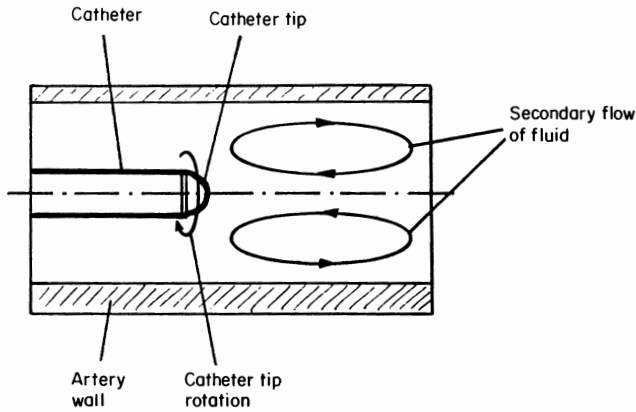


Figure 8 Cross-sectional schematic view of Kensey catheter in artery showing secondary flow vortices

recirculates fluid. *Figure 8* shows the secondary flow. These fluid dynamic effects develop because the catheter tip acts as a viscous pump, a device consisting of a large disc which, when spinning is a viscous fluid, draws fluid axially towards its centre while directing fluid radially away at the base due to centrifugal forces¹⁰. *Figure 9* shows a schematic of the viscous pump effect. At the cylinder walls, the flow is deflected either distal or proximal to the catheter tip. As some of the fluid moves distally, it is drawn back by the viscous pump effect. The resulting flow, i.e., the second fluid dynamic effect, is a vortex along the longitudinal axis which precipitates recirculation of the ambient fluid.

Particles are dragged along with the fluid by viscous effects and in general move with the streamlines of the flow. The force necessary to move particles with the fluid is created by hydrodynamic drag. In the flow surrounding the catheter tip, the predominant velocity component is circumferential. As a consequence, particles have a tendency to rotate around the catheter rather than move axially or radially. Near the catheter tip, the radial velocity is greatest because of fluid moving away from the tip by the centrifugal effect and because of outward perfusate flow exiting radially in this region. For this reason, particles initially drawn toward the tip by the

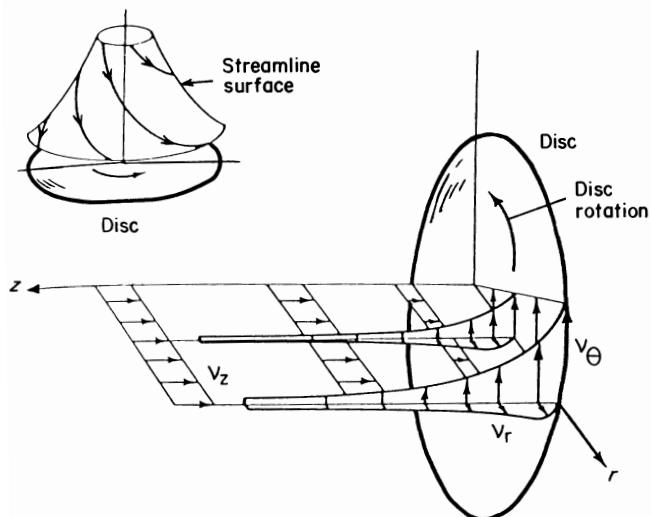


Figure 9 Streamlines directed toward spinning disc showing viscous pump effect¹⁰

viscous pump effect tend to be pushed radially away when they start to spin (see (*Figure 9*)). For particles larger in diameter than the distance between the tip and the lumen, interaction with the tip is unavoidable; particles smaller in diameter than that distance may escape mechanical interaction. These conclusions assume that the catheter is not located eccentrically within the cylinder and that the artery is cylindrical. In general, not all free-floating particles interact mechanically with the catheter tip.

A classical way to characterize fluid flow is to report a non-dimensional number, the Reynolds number, defined as the ratio of the inertial forces to the viscous forces. The Reynolds number for the rotational flow at the catheter tip is large (3700), signifying that the inertial forces are small compared to the viscous forces and implying that the flow is laminar. Calculation of the Reynolds number is presented in the Appendix. Also shown in the Appendix are power calculations suggesting that the power dissipated by viscous effects at the rotating tip through shear stress is small relative to the power required to torsionally fail the catheter.

EXPERIMENTAL OBSERVATIONS

Actual catheter experiments: gelatin model

In the actual size experiments using model occlusions, the generation of particulate debris was evident. Particles were sheared away more visibly with the side edges of the tip than with the forward cutting edge. Particles generated using gelatin as a model for atheroma were often macroscopic with volumes estimated to be between 1 and 5 mm³, compared to the catheter tip with a volume of 7 mm³. Particles were also generated by the shearing action of the catheter sleeve passing through a model occlusion, since experimental catheters had not been pre-lubricated (it is reported that a coating is applied to manufactured product that optimizes the lubricity of the catheter and reduces thrombogenicity in blood). It was generally observed that forcing the catheter through a model occlusion using a clinically recommended procedure of one thrust, generated fewer particles than probing, i.e., alternately advancing and retracting the catheter axially. When made to pass through a model occlusion several times, the non-lubricated catheter broke off many particles because of friction at the walls of the recanalized occlusion. This frictional resistance of the catheter sleeve moving through model occlusions was sensed by the operator who compensated by decreasing the feed rate. In one experiment using a silicon sealant occlusion, the catheter embedded itself in the surrounding tygon tubing and eventually perforated the wall when the operator, who mistakenly believed that the catheter was overcoming frictional resistance, substantially increased the feed force.

Particles were also generated from pressure effects in unpenetrated model occlusions. It was observed that the catheter often burst through model occlusions or disintegrated them before it mechanically removed material. When the catheter reached the distal end of an occlusion, material burst away leaving a stream of particles drifting distally. The effect was particularly

noticeable with the gelatin models where the drifting particles were often large. In contrast to model occlusion material bursting, fracture often occurred in gelatin before the tip completely penetrated the model occlusion. Large sections of the model occlusion separated from the model and passed downstream. It was observed that the injection of fluid contributed to a pressurization at the tip when inside the occlusion causing the model occlusion to burst or fracture. In cases where the catheter met frictional resistance, perfusate injection at the tip caused a bubble to form stretching the occlusion material apart and generating fracture lines.

Because of fluid dynamic effects, the catheter tip attracted stray particles, but in many instances did not mechanically interact with them. After the catheter tip had passed completely through a model occlusion, particulate drawn toward the tip was accelerated radially away. Particles generated from gelatin occlusions were macroscopic and not emulsified. Yet, the viscous pump effect was observed: many particles drifting downstream were drawn back toward, but not struck by, the catheter tip after it had passed through a model occlusion. This effect was particularly evident with smaller particles, which were 1 to 5 mm³ in volume, that were located distally from the tip as far as 50 mm. In many video recordings, larger particles (approximately 5 to 10 mm³) were not impinged by the catheter tip. They broke away from the model occlusion and rotated around the catheter tip in the primary flow vortex approximately 1 mm distal to the tip. When the spinning catheter tip was retracted through the model occlusion, particles separated from the primary flow vortex and drifted downstream owing to the restored flow. Some particles were dragged back through the occlusion sustaining their trajectory in rotation owing to viscous forces. In these experiments, there was little evidence of recirculation of model particulate at the tip.

Actual catheter experiments: fibrous material

In cases where the catheter was introduced in highly fibrous occlusion material, such as minced beef fat, the tip snagged and stopped rotating. In these situations, the torque exerted on the catheter tip by entanglement caused the drive cable to fail in torsion. In addition to inducing torsional failure, fibre can collect around the catheter tip. In one instance, in which the catheter was introduced in a cadaver artery, fibrous material was observed to have wrapped around the sleeve. Although the fibres did not become entangled around the tip and did not cause the cable to fail, they could have drifted downstream when the catheter tip stopped rotating. The results of these observations suggest that the catheter may have difficulty operating in the presence of fibre, a component of some atheromatous material.

10x Scale catheter experiments

The 10 × scale model tests were organized to provide better visualization of fluid flow and particle interaction around the catheter tip. In these tests, model particles were introduced proximally from the upper tank to trace fluid flow and monitor recirculation. As

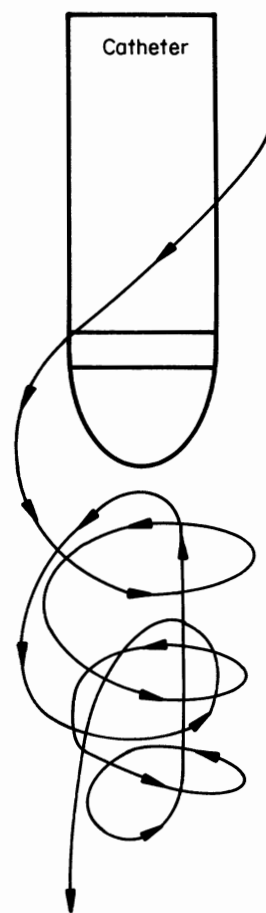


Figure 10 Path of particle caught in spiral and recirculated near catheter tip

particles floated down the visualization chamber, they rotated increasingly with the primary flow as they approached the catheter tip. In situations where the model catheter was positioned eccentrically in the chamber, near the wall of the tube, tracer particles were least influenced by the fluid dynamic effects mentioned. Few particles were drawn back to the tip or even displaced tangentially. When the tip was located centrally within the visualization chamber some recirculation was observed. In this case, particles were observed to be caught in a spiral and drawn back to the tip where they were redirected away only to return when caught back in the onrush of flow, see *Figure 10*. A zone was established distal to the tip where descending particles were recirculated and outside which they passed without being drawn to the tip. The zone was larger when the catheter operated with no fluid injection than when injection was used. When the catheter was positioned against the visualization chamber wall, the zone size was negligible. These studies suggest that both eccentricity of the catheter within the artery and the perfusate injection diminish the catheter's ability to recirculate particulate.

CONCLUSIONS

To elucidate the mechanism by which the catheter revascularizes atheromatous arteries, *in vitro* experiments with actual and 10 × scale model Kensey catheters were performed.

The findings of this work suggest that in recanalizing gelatin model occlusions, the catheter generates particulate debris in three ways: the catheter can break up material with the side edges of the rotating tip, it can shear away particles from occlusion material by friction generated at the surface of the catheter sleeve, and it can dissect the occlusion through pressure effects. Particles thus generated are recirculated by viscous effects, such as flow vortices at the catheter, which can attract particles to the tip or rotate particulate debris around the catheter tip. However, such effects do not necessarily redirect the particles for subsequent impingement by the tip. Perfusate output and a net radial acceleration of surrounding fluid at the tip further impede mechanical interaction of particulate with the tip.

In summary, several mechanisms have been identified by which the Kensey catheter breaks up material. These mechanisms may occur during use of the catheter for revascularization. However, the purpose of this study was to analyse the fluid dynamic and mechanical effects of the Kensey catheter during its interaction with simulated atheroma material.

ACKNOWLEDGEMENTS

The authors are grateful to several key individuals: Dr Mark B. Friedman of the Robotics Institute, Carnegie Mellon University, Pittsburgh, Pennsylvania for many helpful suggestions during the course of this research, especially his indispensable aid in designing the test equipment; Mr James Dillinger of the Department of Mechanical Engineering, Carnegie Mellon University, Pittsburgh, Pennsylvania for his mechanical expertise and machining; Mr Tom Bales and Ms Enora Rogers, Theratek International Inc., Miami Lakes, Florida for their guidance and engineering support. In addition, the authors gratefully acknowledge the financial support of Theratek International, Inc., Miami Lakes, Florida and the services of the Department of Radiology, Shadyside Hospital, Pittsburgh, Pennsylvania.

REFERENCES

1. Utley J, Carlson EL, Hoffman JIE, Martinex HM and Buckberg GD. Total and regional myocardial blood flow measurements with 25 μ , 15 μ , 9 μ and filtered 1–10 μ diameter microspheres and antipyrine in dogs and sheep. *Circulation Research* March 1974, **34**: 391–9.
2. Summary of clinical experience with the Kensey catheter in Europe. Document 2E-800-0164-1, *Cordis International SA*, September 1989.
3. Commonly asked questions about the Kensey catheter. Document 151-5725-1, *Cordis Corporation*, September 1988.
4. Coleman CC. Atheroablation with the Kensey catheter: a pathologic study. *Radiology*, 1989; **170**: 393–40.
5. Kensey KR. Recanalization of obstructed arteries with a flexible, rotating tip catheter. *Radiology*, 1987; **165**: 387–9.
6. Fung YC. *Biomechanics: Mechanical Properties of Living Tissues*. New York: Springer-Verlag, 1981; 63–7.
7. Wholey MH. Advances in balloon technology and perfusion devices for peripheral circulation. *American Journal of Cardiology*, 1988; **61**: 87G–95G.
8. Kensey KR. Recanalization of obstructed arteries with a flexible, rotating tip catheter. *Radiology*, 1987; **165**: 387–9.

9. Instructions for use: 8 French Kensey catheter. Document # 0001432B, *Theratek International Inc., Miami Lakes, Florida*, December 16, 1987.
10. Panton RL. *Incompressible Flow*. New York: John Wiley & Sons, 1984, 296.
11. Fung YC. *A First Course in Continuum Mechanics*. Englewood Cliffs: Prentice-Hall, NJ, 1977, 233.
12. White FM. *Viscous Fluid Flow*. New York: McGraw-Hill, 1974, 117–18.
13. Hughes WF, Gaylord EW. *Basic Equations of Engineering Science*, Schaum's Outline Series. New York: McGraw-Hill, 1964.

APPENDIX

The Kensey catheter rotating in a blood vessel is modelled as a system of concentric cylinders. The inner cylinder, representing the catheter tip, is assumed to rotate at a steady angular speed ω_0 and has radius r_0 . The outer cylinder, representing the vessel, is assumed fixed and has radius r_1 .

Reynolds number calculation

The Reynolds number, Re , is defined as

$$Re = \frac{\rho L \nu_m}{\mu}$$

where the density of the fluid is ρ , the characteristic length L is the gap ($r_1 - r_0$), ν_m is the mean velocity and μ is the coefficient of viscosity of the fluid (blood). Here the mean velocity is taken as half of the tangential velocity component at the inner cylinder. Thus, the Reynolds' number is

$$Re = \frac{\rho(r_1 - r_0) r_0 \omega_0}{2\mu}$$

Assuming the following representative numbers: $r_0 = 1.33$ mm, $r_1 = 4.00$ mm, $\omega_0 = 100\,000$ rpm = $10\,500$ rad s⁻¹, $\rho = 993$ kg m⁻³ (density of water at 37°C), and $\mu = 5.0 \times 10^{-3}$ N s m⁻² (blood)¹¹, the Reynolds' number is 3700. Hence, the flow is modelled as laminar, since the Reynolds' number is larger than 2000, the Reynolds' number associated with the transition from laminar to turbulent flow.

Power calculations

From the continuity equation and the tangential component of the momentum equation it can be shown¹² that the tangential component of velocity, ν , at radius r is

$$\nu = r_0 \omega_0 \left(\frac{r_1^2}{r_0 r} - \frac{r}{r_0} \right) / \left(\frac{r_1^2}{r_0^2} - 1 \right)$$

Since this tangential velocity component is the only non-zero component (in this simplified model), it follows that the shear stress τ can be written

$$\tau = \mu \left(\frac{d\nu}{dr} - \frac{\nu}{r} \right)$$

where μ is the coefficient of viscosity¹³. Evaluating the shear stress at the inner rotating cylinder, $r = r_0$, gives

$$\tau = \mu \left(\frac{d\nu}{dr} \Big|_{r=r_0} - \omega_0 \right)$$

from which it follows:

$$\tau = \frac{2\mu\omega_0}{\left(\frac{r_0^2}{r_1^2} - 1\right)}$$

The power dissipated through the action of this shear stress is

$$P = \tau r_0 A \omega_0$$

where the surface area, A , is

$$A = 2\pi r_0 d$$

where d is the axial distance of the rotating inner cylinder. Combining terms, the expression for

dissipated power is

$$P = \frac{4\pi\mu r_0^2 \omega_0^2 d}{\left(\frac{r_0^2}{r_1^2} - 1\right)}$$

In particular, using the numbers above the dissipated power is 28 mW with $d = 2$ mm. This power is very small relative to the power required to torsionally fail the cable, i.e.,

$$\begin{aligned} P_{\max} &= T_{\max} \omega_0 \\ &= (7.2 \times 10^{-3} \text{ N m})(10\,500 \text{ rad s}^{-1}) \\ &= 76 \text{ W} \end{aligned}$$

where $T_{\max} = 7.2 \times 10^{-3}$ N m is the torque associated with cable failure, as reported by the manufacturer.